Supplement of Earth Surf. Dynam., 10, 23–42, 2022
https://doi.org/10.5194/esurf-10-23-2022-supplement

Earth Surface Dynamics
Open Access
EGU

Supplement of

Intensified paraglacial slope failures due to accelerating downwasting of a temperate glacier in Mt. Gongga, southeastern Tibetan Plateau

Yan Zhong et al.

Correspondence to: Qiao Liu (liuqiao@imde.ac.cn)

Supplemental Figures

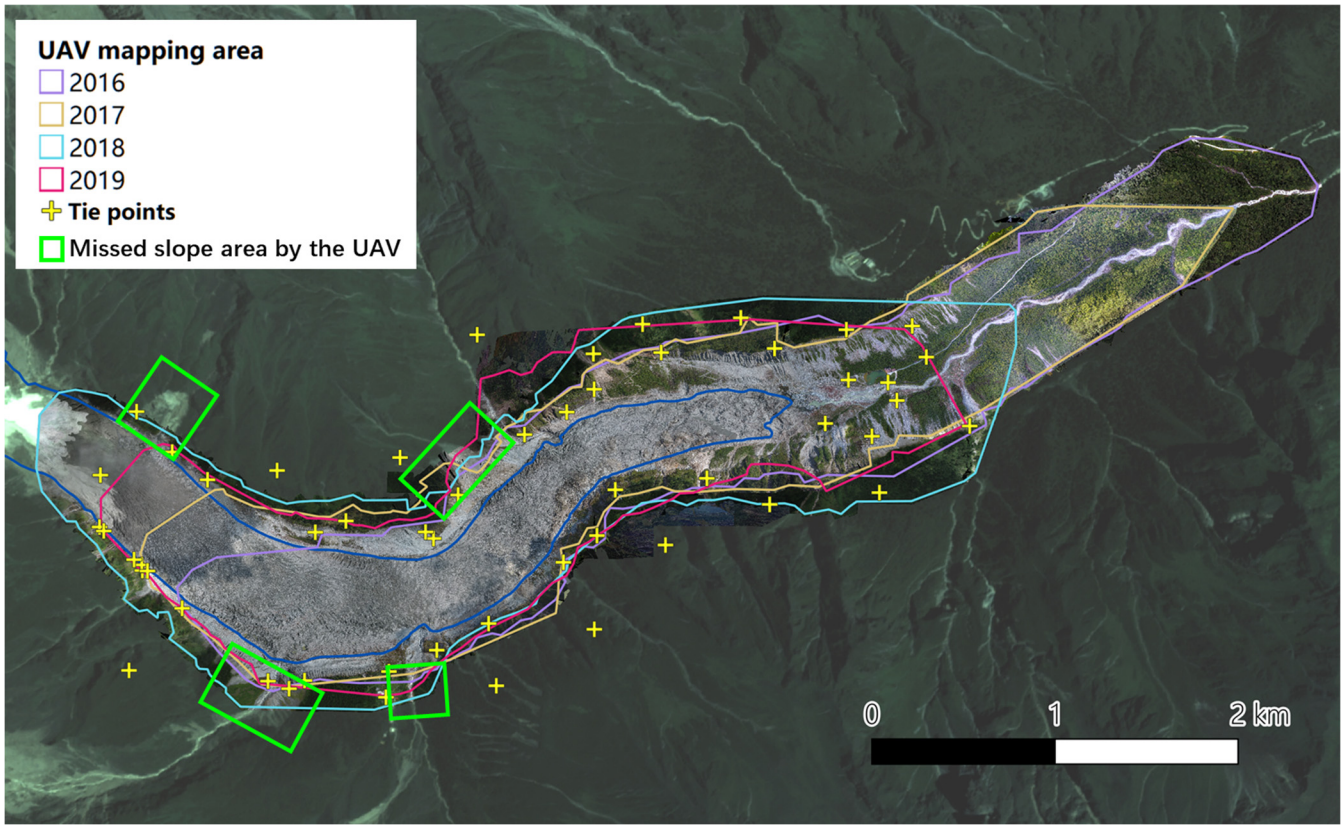

Fig. S1: Spatial extents of the four repeated UAV surveys by Qiao Liu et al. and the distribution of tie points selected for imagery co-registration. Note the 'tie points' outside the UAV mapping areas were only used for extrapolation but not for co-registration.

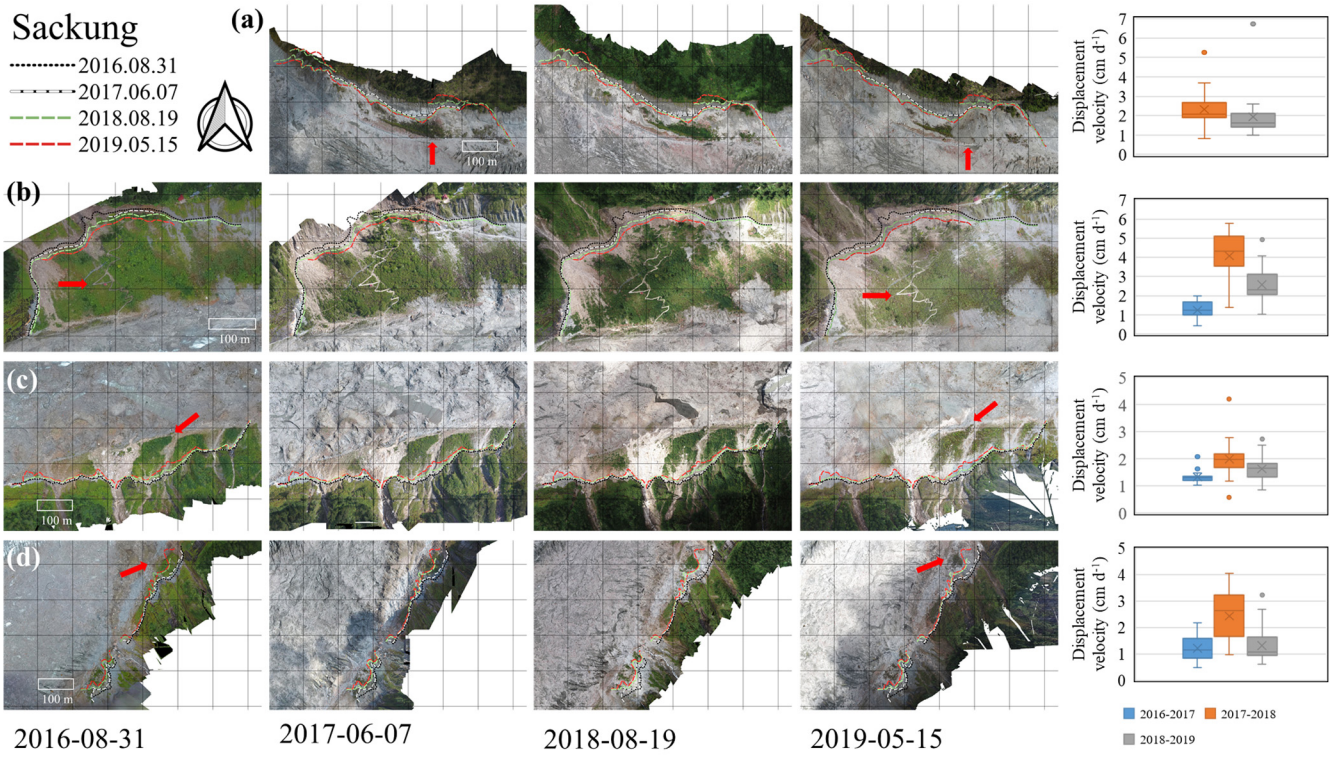

Figure S2: Slopes slides and its velocity of type B. (a) B1, (b) B2, (c) B3, (d) B4 based on UAV images.

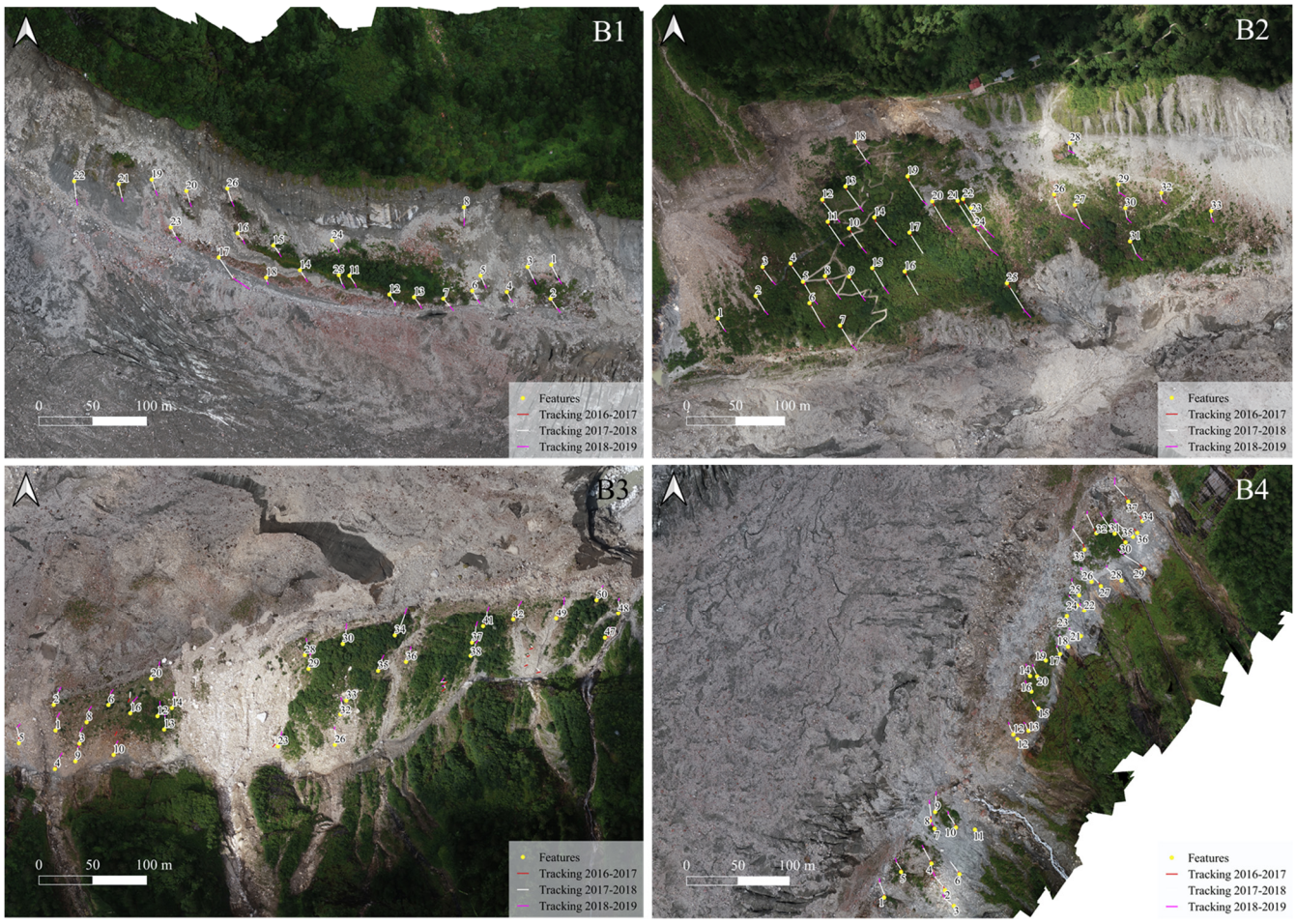

Fig. S3: Tie points for manually tracked the displacement of the four slopes (B1-B4 in Fig. 6) in UAV imagery.

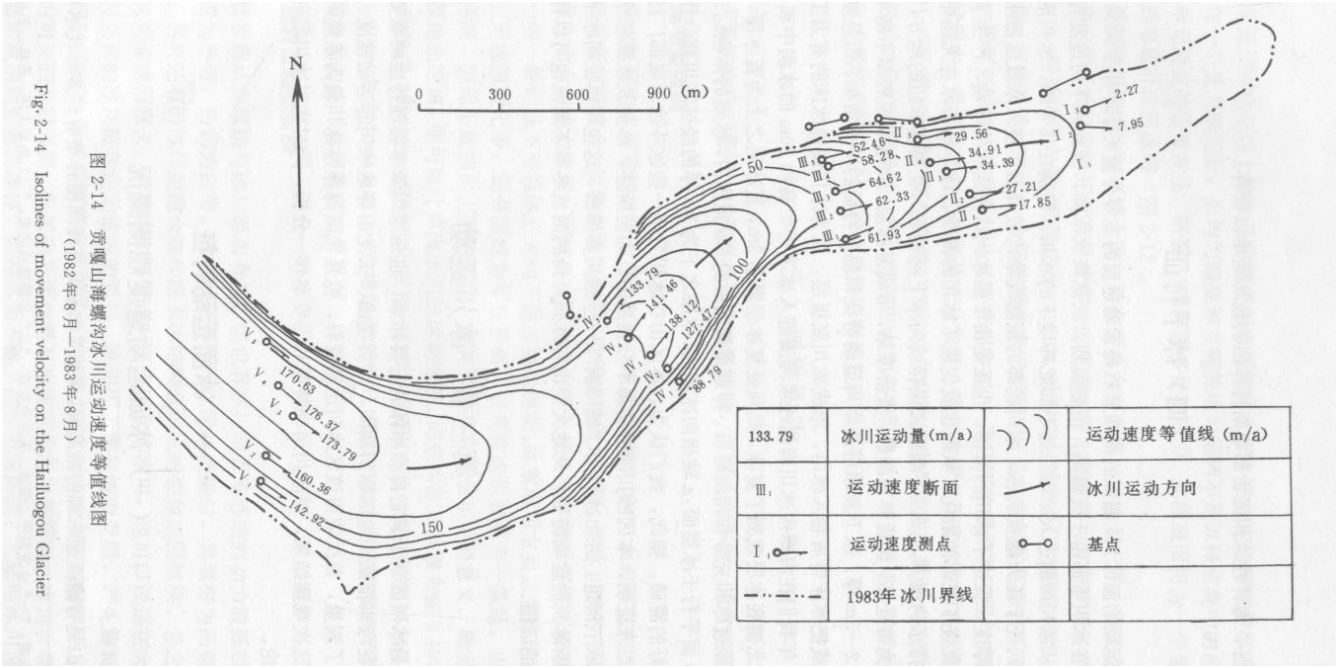

图 2-14 贡嘎山海螺沟冰川运动速度等值线图
(1982年8月—1983年8月)

Fig. 2-14 Isolines of movement velocity on the Hailuogou Glacier

Fig. S4: The scanned picture of HLG velocity between 1982 and 1983.

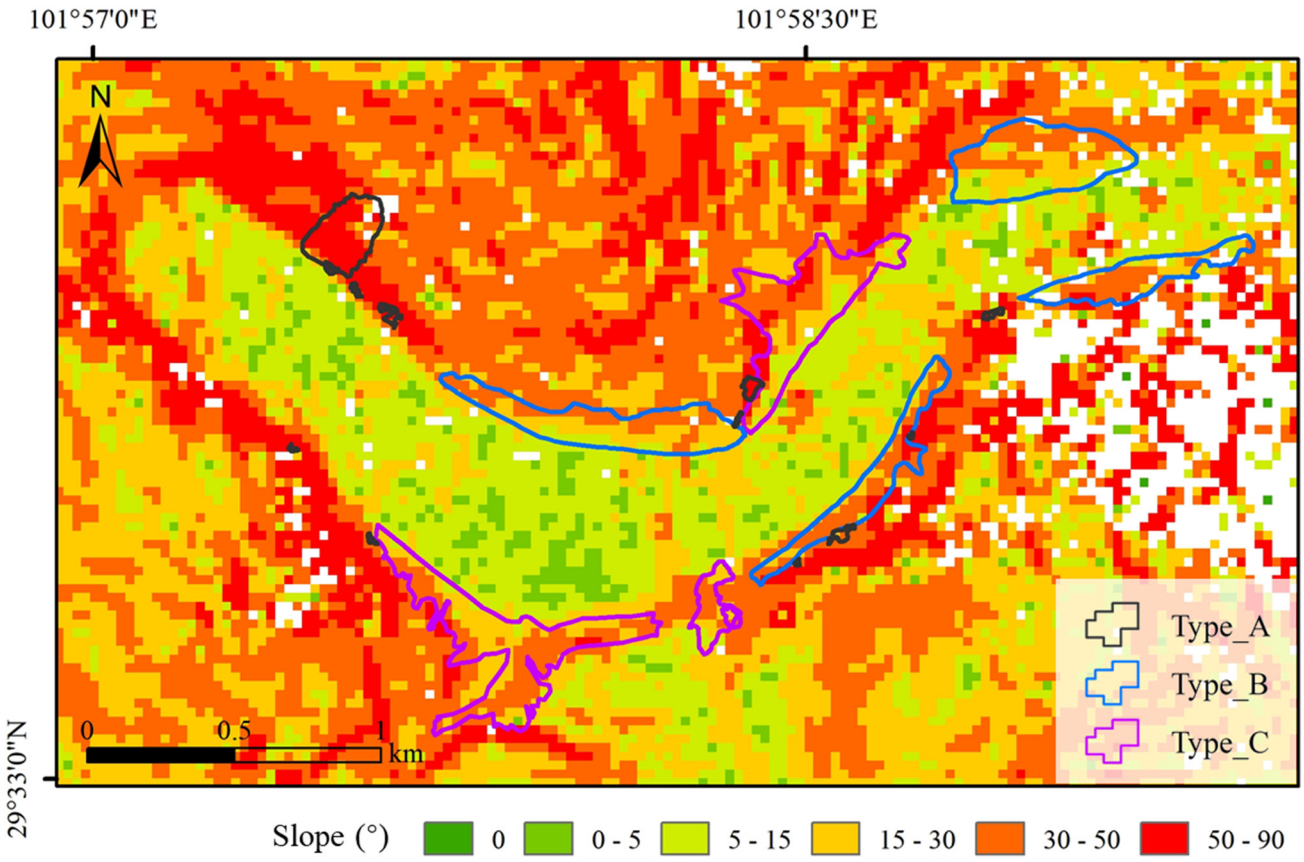

35 **Fig. S5: Surface gradient map based on the 2016 DEM derived using 2000 SRTM and the 2000-2016 surface elevation change rate from Brun et al. (2017).**

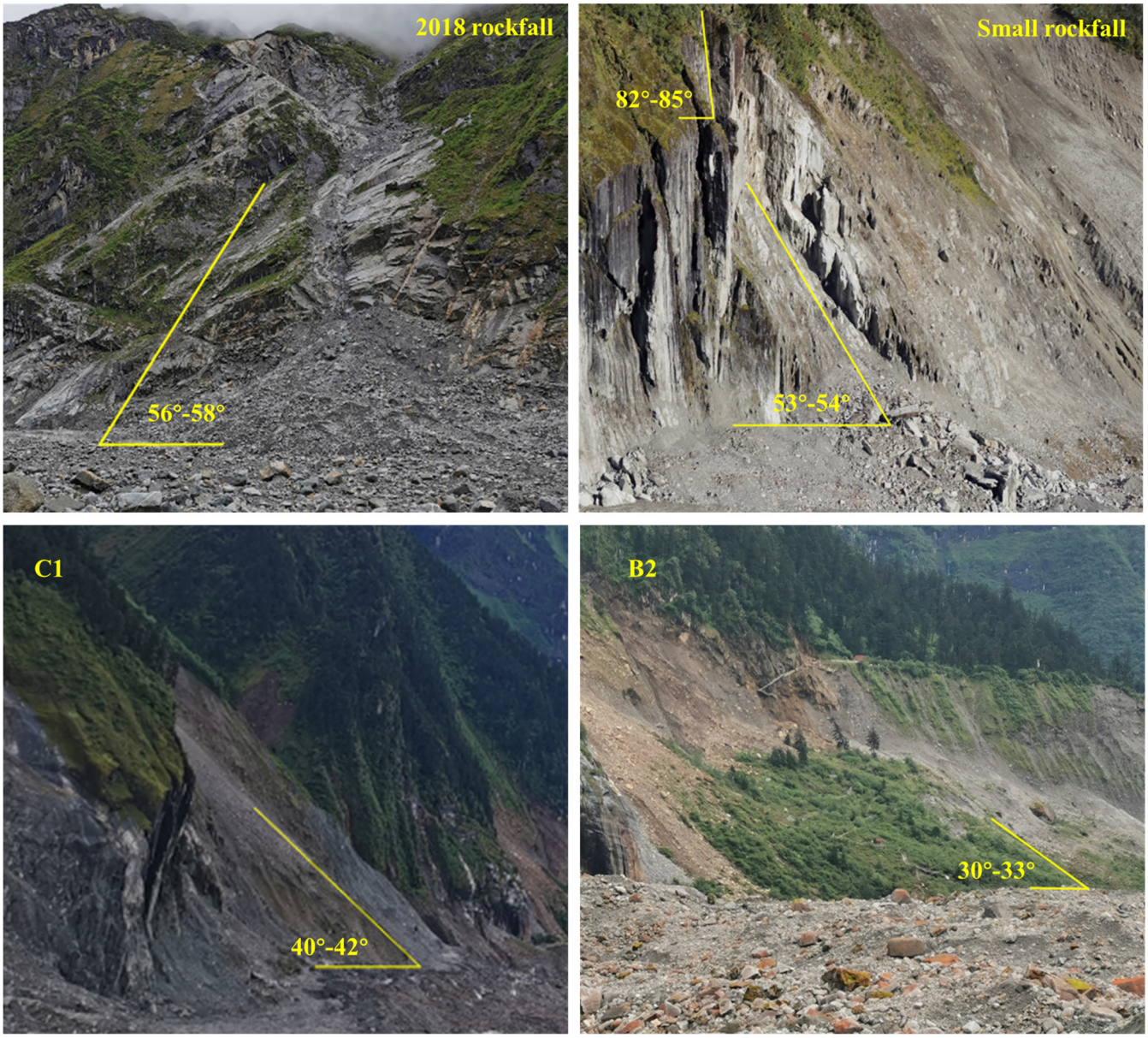

Fig. S6: The slope angles of some PSF in field investigation, photographs by Yan Zhong.

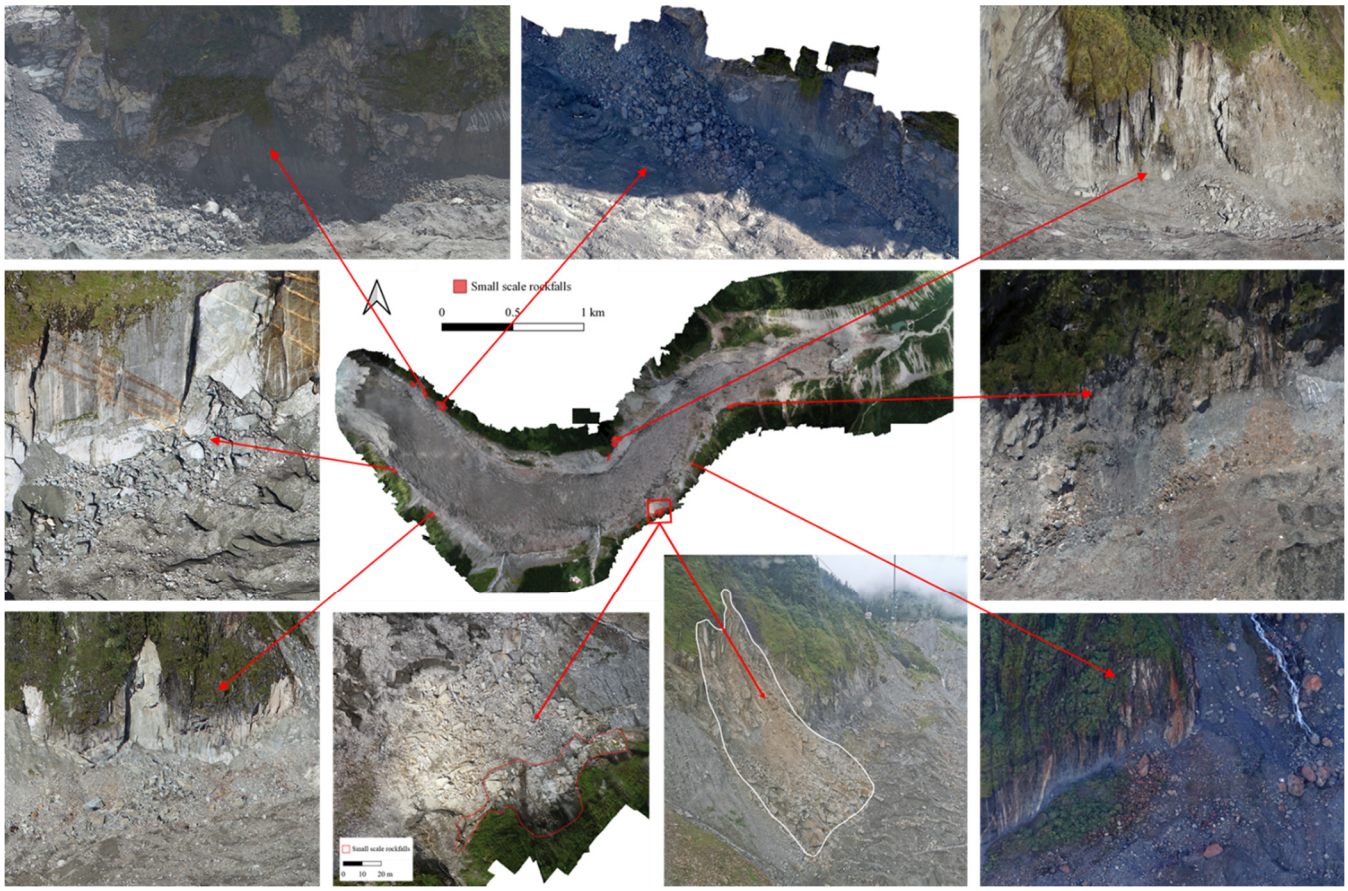

Fig. S7: Detected small magnitude rockfalls from UAV- and field-photographs.

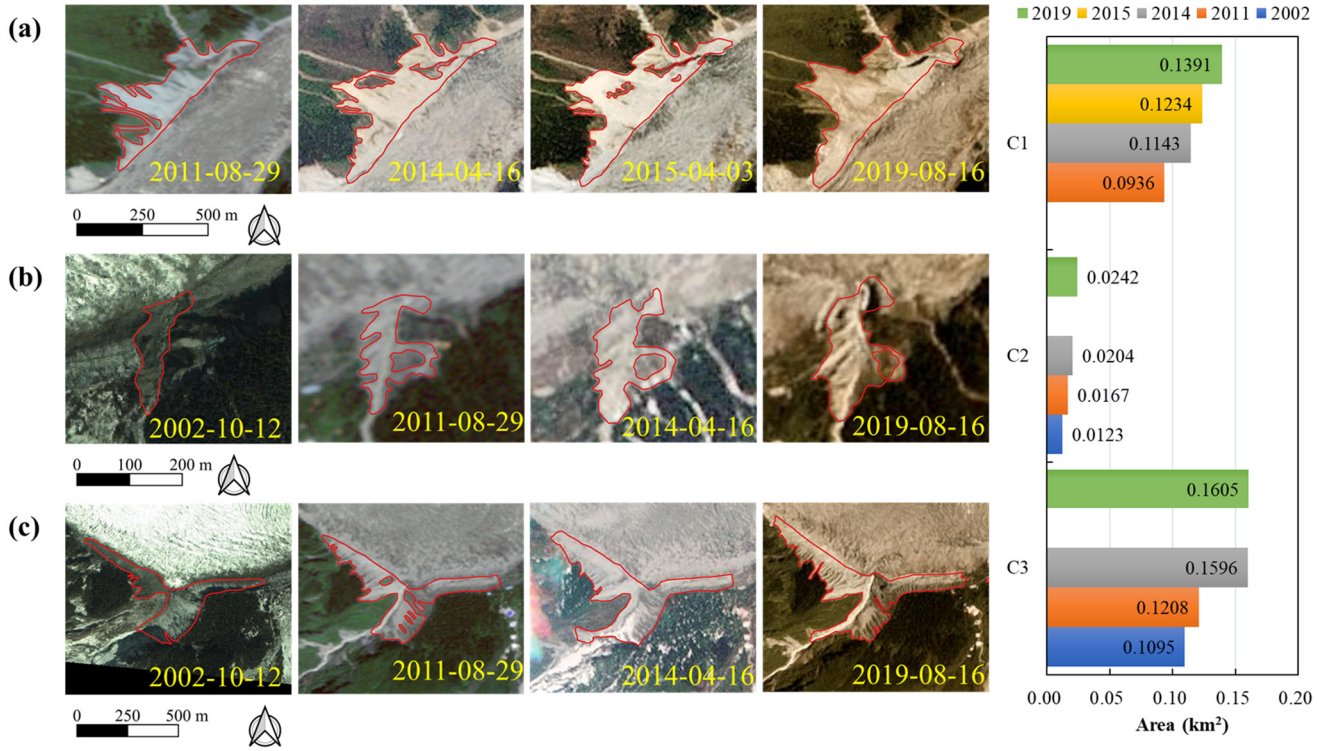

Fig. S8: Slopes range and area changes of type C. (a) C1, (b) C2, (c) C3 based on RapidEye, PlanetScope and © Google Earth (SPOT5) images.

Fig. S9: Glacially smoothed and polished bedrock surfaces with steep inclination angles in B1 and its opposite bank, photographs by Yan Zhong.

50

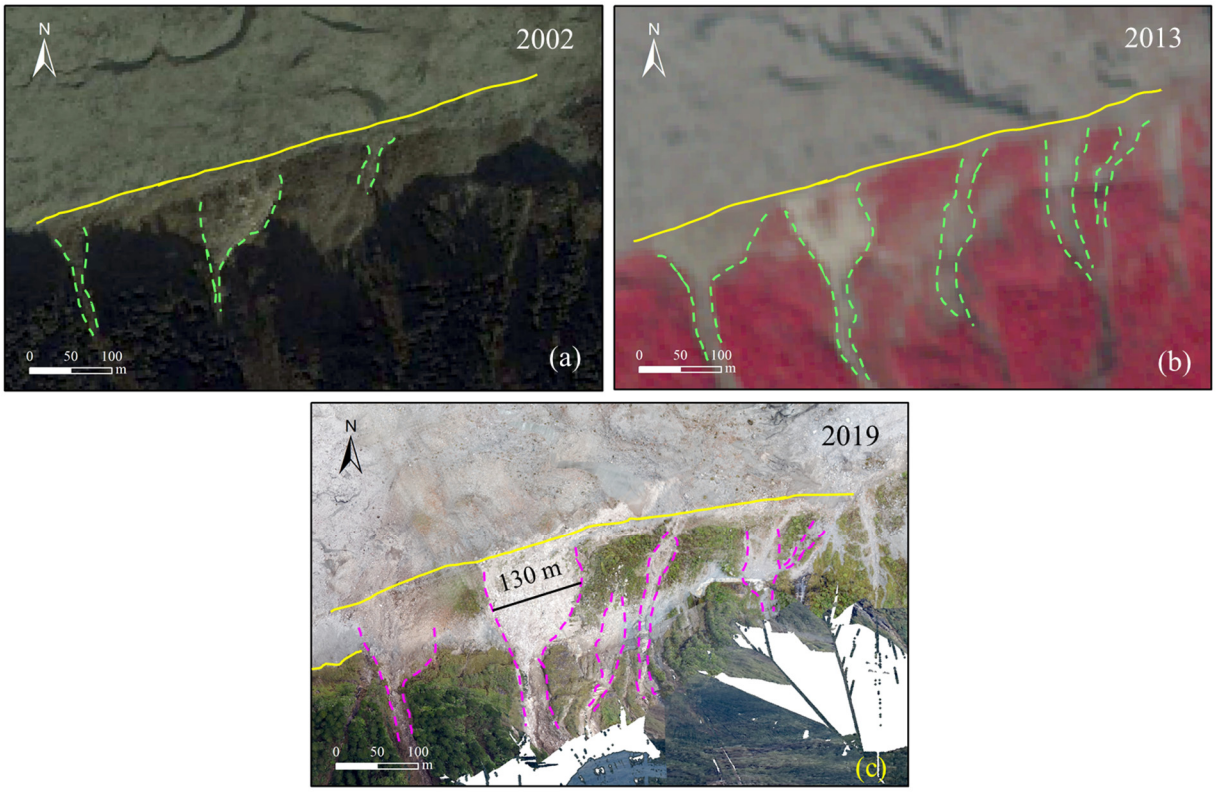

Fig. S10: The gully developing process within B3 between 2002, 2013, and 2019, UAV imagery by Qiao Liu et al.

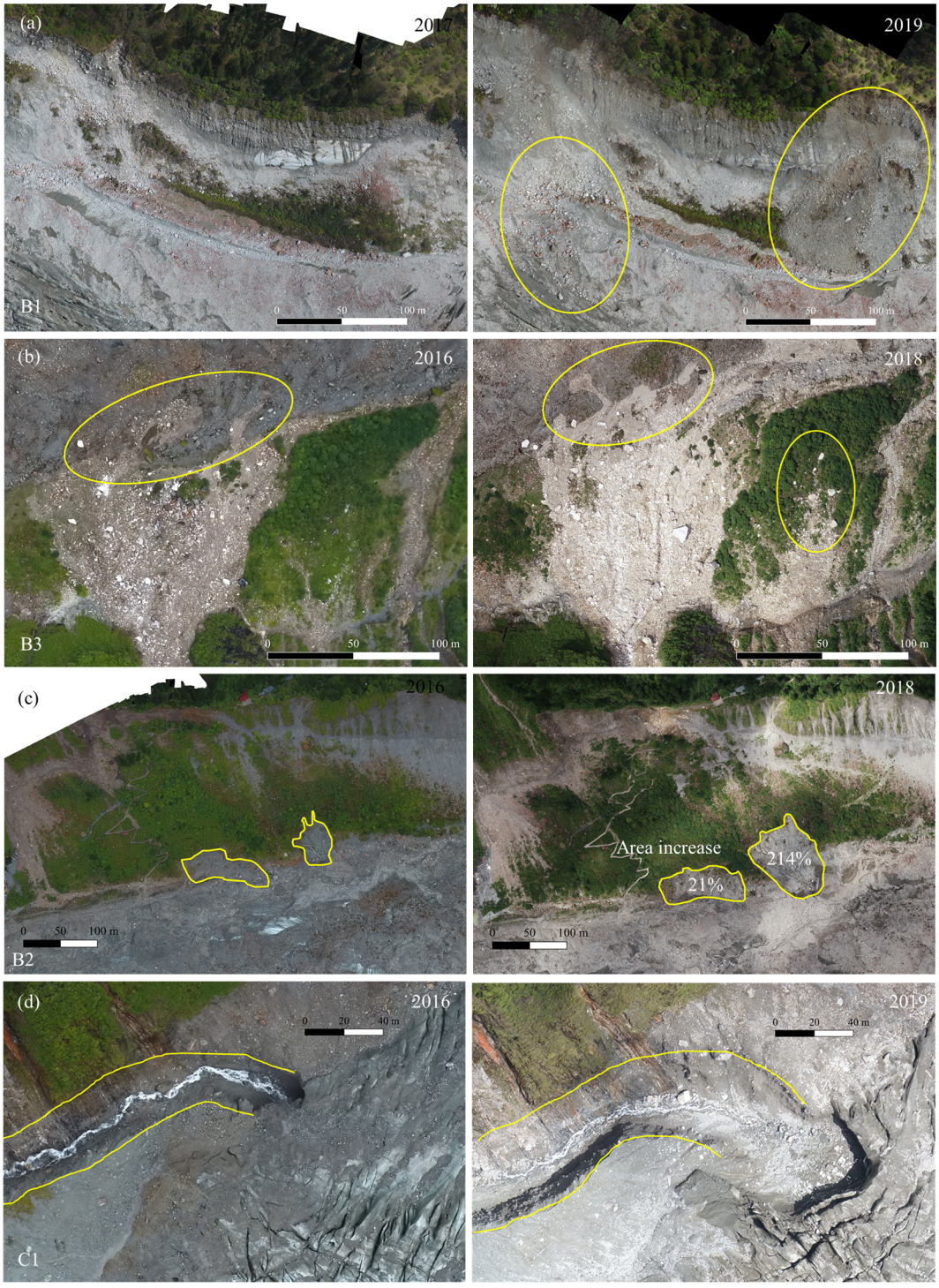

55 **Fig. S11: A limited number of materials that are delivered to the supraglacial or sub-glacial environment through (a) direct rolled (the sediments are more dispersed compared to rockfalls), (b) collapse, (c) debris flow (faster changes), and (d) stream, UAV imagery by Qiao Liu et al.**

Supplemental Table

Tab. S1 PSF classification

Categories		Sub-categories		Classification Standard	Classification Result
ID	Name	ID	Name		
1.0	Rock slope failure	1.1	Rock avalanche	Large-scale, catastrophic rock slope failure Volume class: $\geqslant 10^6$ (m^3) (Deline et al., 2015)	-
		1.2	Rock fall	Local-scale, high-frequency, and discrete rockfalls Volume class: $\leqslant 10^6$ (m^3) (McColl, 2012)	A
		1.3	Deep-seated gravitational slope deformations	Extremely slow flows or displacements of bedrock (McColl, 2012)	-
2.0	Sediment slope failure	2.1	Sediment-mantled slope slide	Rock mass slides along the shear plane Shape: arc or strip (Ballantyne, 2002;Cody et al., 2020;Hungr et al., 2014)	B1-B4
		2.2	Gulley headward erosion	Strong headward erosion is added based on Type 2.1 Shape: triangle	C1-C3

References

Ballantyne, C. K.: Paraglacial geomorphology, Quaternary Science Reviews, 21, 1935-2017, doi:10.1016/S0277-3791(02)00005-7, 2002.

Cody, E., Anderson, B. M., McColl, S. T., Fuller, I. C., and Purdie, H. L.: Paraglacial adjustment of sediment slopes during and immediately after glacial debuttressing, Geomorphology, 371, 107411, doi:10.1016/j.geomorph.2020.107411, 2020.

Deline, P., Hewitt, K., Reznichenko, N., and Shugar, D.: Chapter 9 - Rock Avalanches onto Glaciers, in: Landslide Hazards, Risks and Disasters, edited by: Shroder, J. F., and Davies, T., Academic Press, Boston, 263-319, 2015.

Hungr, O., Leroueil, S., and Picarelli, L.: The Varnes classification of landslide types, an update, Landslides, 11, 167-194, doi:10.1007/s10346-013-0436-y, 2014.

McColl, S. T.: Paraglacial rock-slope stability, Geomorphology, 153-154, 1-16, doi:10.1016/j.geomorph.2012.02.015, 2012.